Uli Haisch, MPI Munich
Workshop on Tools for High Precision LHC Simulations, 2.11.22

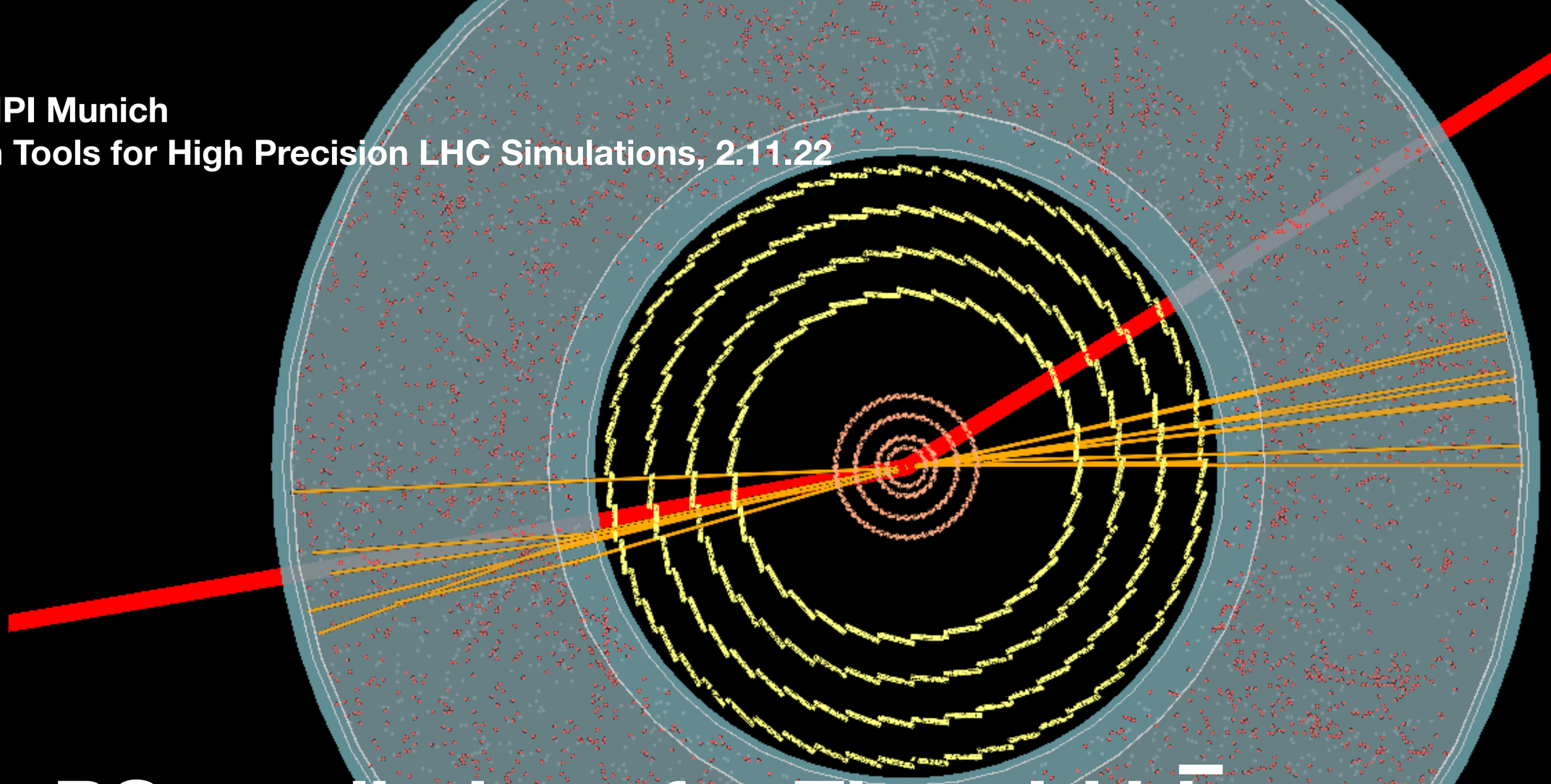

NNLO+PS predictions for $Zh \to l^+l^- b\bar{b}$ production in SMEFT

Observation of h → bb̄ @ LHC Run II

[ATLAS, 1808.08238]

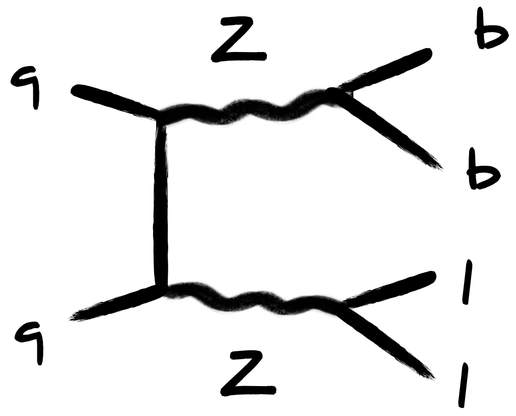

background

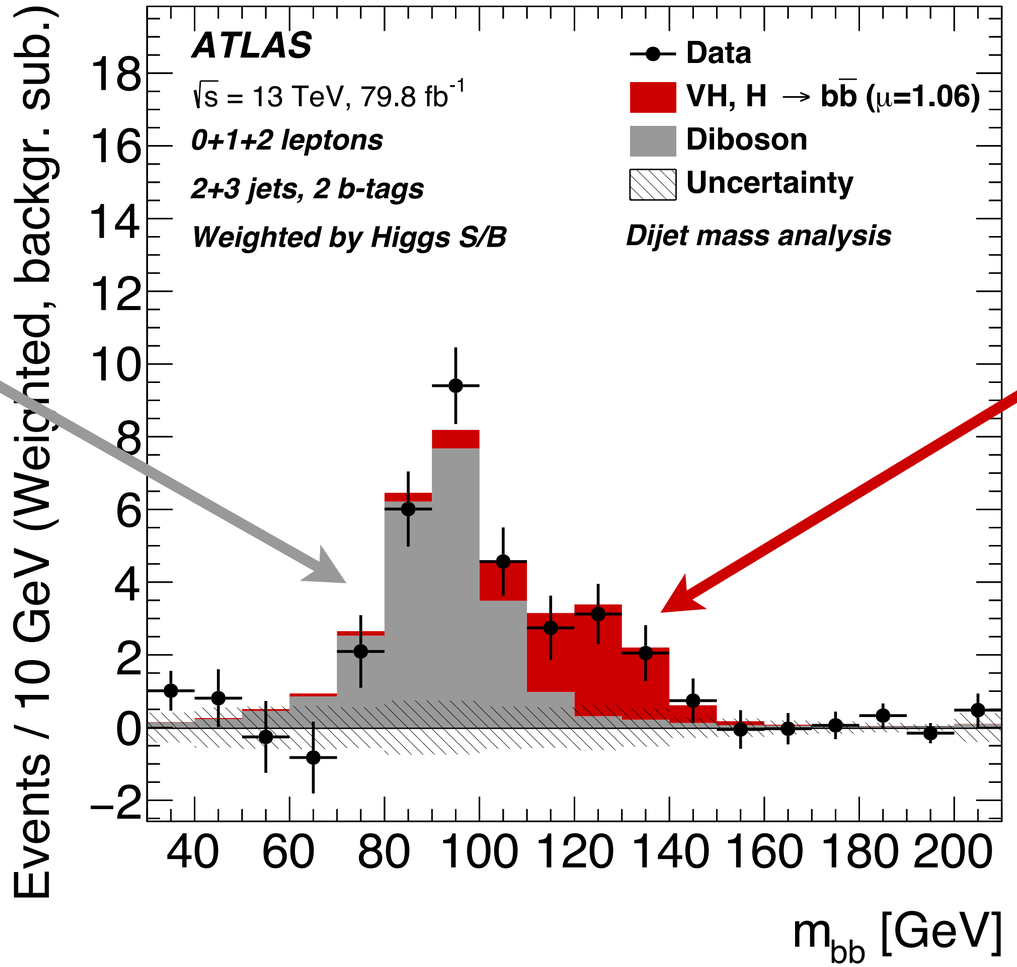

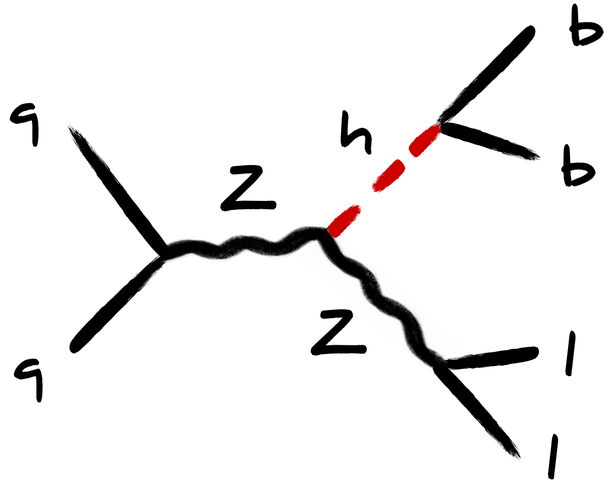

signal

[see also CMS, 1808.08242]

From 5σ to precision measurements

[ATLAS, 1808.08238]

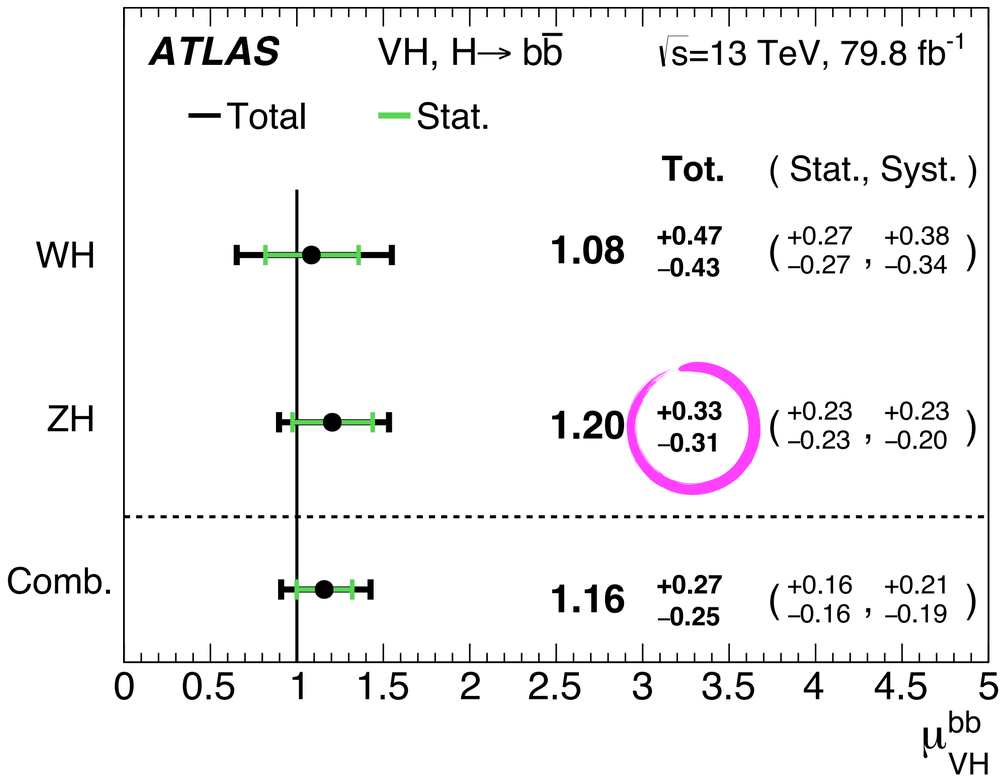

In LHC Run II, signal strength in Vh production found to be SM-like within 25%

[see also CMS, 1808.08242]

From 5σ to precision measurements

[ATLAS, 1808.08238]

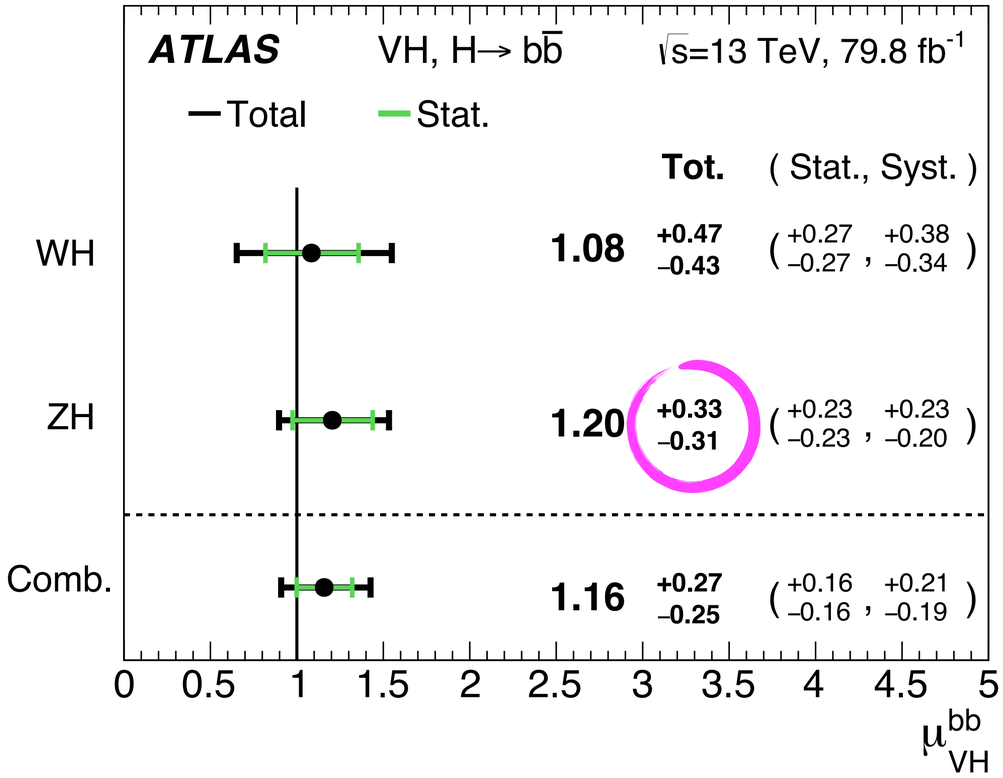

[ATL-PHYS-PUB-2018-054]

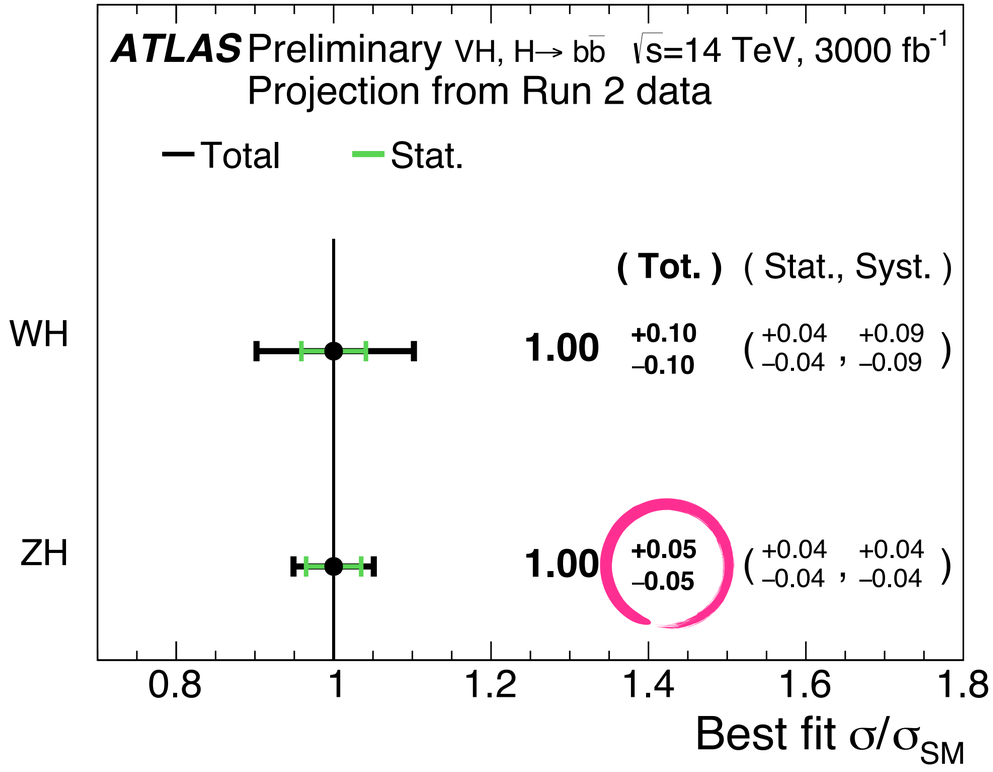

Ultimate accuracy projected to be 10% to 5% in Wh & Zh channel @ HL-LHC

[see also CMS, 1808.08242; CMS-PAS-FTR-18-011]

Anatomy of SMEFT effects

corrections to $q\bar{q}Z$ & $q\bar{q}Zh$ vertices

[Greljo et al., 1710.04143; Alioli et al., 1804.07407; Bishara et al., 2208.11134]

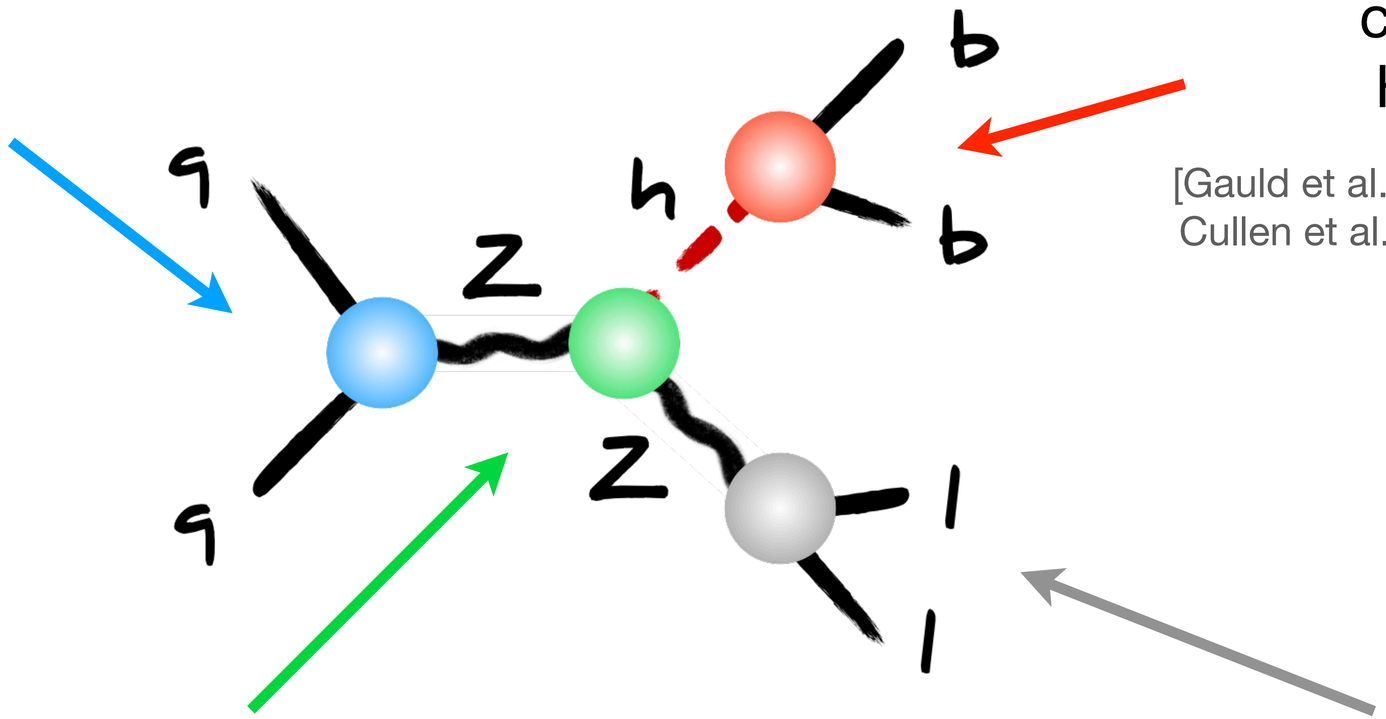

corrections to Higgs decay

[Gauld et al., 1607.0635; Cullen et al., 1904.06358; 2007.15238]

corrections to hZZ vertex

[Maltoni et al., 1311.1829, Mimasu et al., 1512.02572; Degrande et al., 1609.04833; Greljo et al., 1710.04143; Alioli et al., 1804.07407; Bizon et al., 2106.06328]

if EWPO imposed, effects in Z decay negligible

Goal of 2204.00663, …

Within SM, NNLO+PS accuracy has been recently achieved for Zh production with $Z \to l^+l^-$ & $h \to b\bar{b}$

Match this accuracy in SMEFT, so that numerical impact of missing higher-order QCD effects related to dimension-six operators are below 1% once experimental constraints on Wilson coefficients are taken into account

Many SMEFT operators, so first consider subset of operators that directly contribute in QCD; do operators contributing to hZZ, $q\bar{q}Z$ & $q\bar{q}Zh$ vertices later

[for SM calculation see Astill et al., 1804.08141; Alioli et al., 1909.02026; Bizon et al., 1912.09982; Zanoli et al., 2112.04168]

Operators considered in our work

$$Q_{H\Box} = (H^\dagger H)\,\Box\,(H^\dagger H) \qquad Q_{HD} = (H^\dagger D_\mu H)^*\,(H^\dagger D^\mu H)$$

$$Q_{bH} = y_b\,(H^\dagger H)\,\bar{q}_L\,b_R\,H \qquad Q_{bG} = \frac{g_s^3}{(4\pi)^2}\,y_b\,\bar{q}_L\sigma_{\mu\nu}T^a\,b_R\,H\,G^{a,\mu\nu}$$

$$Q_{HG} = \frac{g_s^2}{(4\pi)^2}\,(H^\dagger H)\,G^a_{\mu\nu}G^{a,\mu\nu} \qquad Q_{3G} = \frac{g_s^3}{(4\pi)^2}\,f^{abc}G^{a,\nu}_{\mu}G^{b,\sigma}_{\nu}G^{c,\mu}_{\sigma}$$

Operators normalised such that Wilson coefficients are expected to be of O(1) in UV-complete weakly-coupled BSM models

[UH, Scott, Wiesemann, Zanderighi & Zanoli, 2204.00663]

Factorisable contributions

Since operators $Q_{H\Box}$, Q_{HD} & Q_{bH} do not contain a gluon, associated SMEFT effects factorise to all orders in strong coupling constant. SMEFT results can be obtained from SM matrix elements by following simple replacement:

$$y_b^2 \to y_b^2 \left\{1 + \frac{2v^2}{\Lambda^2}\left[C_{H\Box} - \frac{C_{HD}}{4} - \mathrm{Re}\left(C_{bH}\right)\right]\right\}$$

corrections due to Higgs wave function

correction due to Yukawa operator

[UH, Scott, Wiesemann, Zanderighi & Zanoli, 2204.00663]

Factorisable contributions

For example in case of partial h → b$\bar{\text{b}}$ decay rate factorisable corrections are:

$$\Gamma(h \to b\bar{b})^{\text{fac}}_{\text{SMEFT}} = \frac{3y_b^2 m_h}{16\pi}\left\{1 + \frac{2v^2}{\Lambda^2}\left[C_{H\Box} - \frac{C_{HD}}{4} - \text{Re}\left(C_{bH}\right)\right]\right\}$$

$$\times\left[1 + \frac{\alpha_s}{\pi}5.67 + \left(\frac{\alpha_s}{\pi}\right)^2 29.15\right]$$

NLO & NNLO QCD correction in SM

[in principle extension to N^{4}LO possible using SM results given in Baikov et al., hep-ph/0511063; Herzog et al., 1707.01044]

Non-factorisable contributions

Dominant non-factorisable corrections arise from dipole operator Q_{bG}:

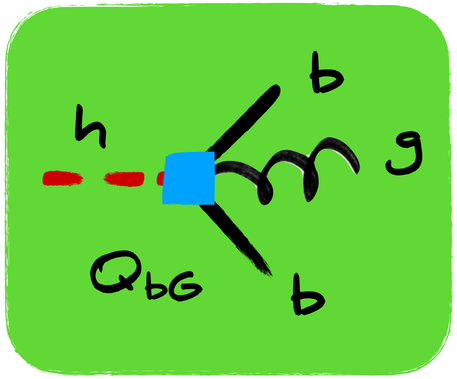

leading contribution from
interference of $h \to b\bar{b}g$
amplitude in SMEFT & SM

[Gauld, Pecjak & Scott, 1607.06354]

Non-factorisable contributions

Dominant non-factorisable corrections arise from dipole operator Q_{bG}:

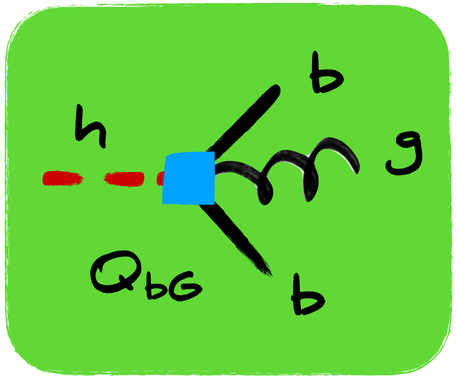

beyond leading order, double real, 1-loop single real & 2-loop virtual contributions

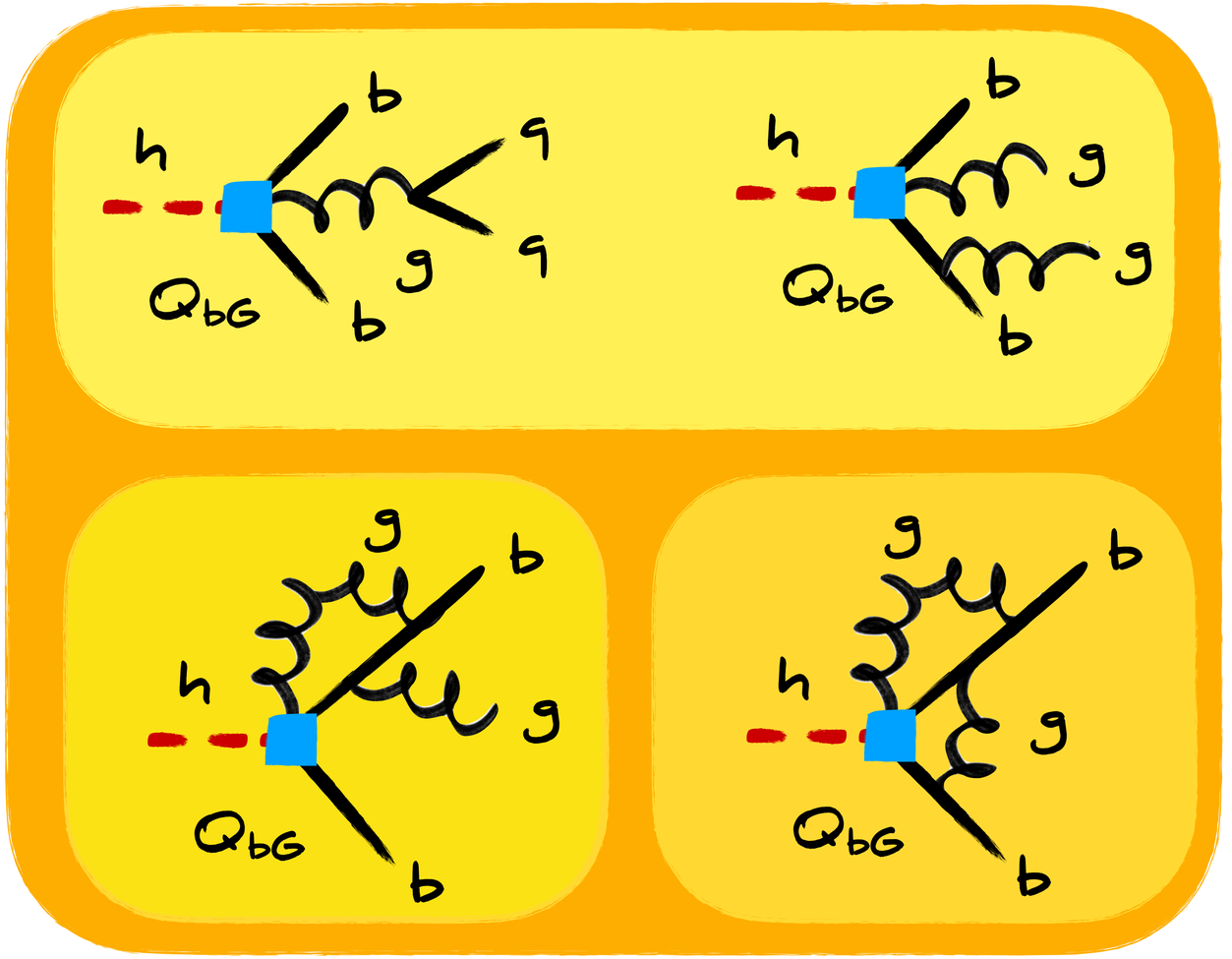

[UH, Scott, Wiesemann, Zanderighi & Zanoli, 2204.00663]

Non-factorisable contributions

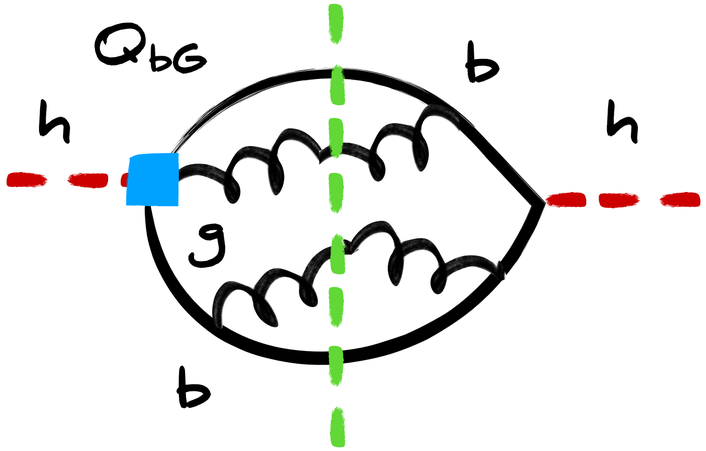

$$f_{b\bar{b}gg}\left(p_1,p_2,p_3,p_4\right) = \frac{4y_{24}^2}{y_{23}y_{34}y_{234}} + \frac{y_{13}^2y_{24}^2}{2y_{14}y_{23}y_{34}y_{134}y_{234}} + \frac{(10}{}$$

$$+ \frac{\left(4y_{24}+19y_{34}-4\right)y_{24}}{y_{23}y_{134}y_{234}} + \frac{\left(4y_{14}\left(y_{23}+2\right)+y_{13}\left(12y_{24}+7\right)\right)}{2y_{34}y_{134}y_{234}}$$

$$- \frac{2y_{34}^2}{y_{13}y_{14}y_{134}} + \frac{y_{34}^2\left(y_{23}+y_{24}+y_{34}-1\right)}{y_{13}y_{14}y_{23}y_{134}} + \frac{y_{34}^2\left(y_{23}+3y_{24}+\right.}{y_{13}y_{14}y_{134}y_{23}}$$

$$+ \frac{18y_{34}+2y_{24}\left(4y_{13}+2y_{23}+2y_{24}+2y_{34}+19\right)-3}{2y_{134}y_{234}} + \frac{12y_{14}}{}$$

$$+ \frac{2y_{14}y_{24}\left(2y_{24}+3y_{34}-1\right)+y_{34}\left(3y_{34}^2+\left(9y_{24}-2\right)y_{34}+4\left(\right.\right.}{y_{13}y_{23}y_{134}y_{234}}$$

[UH, Scott, Wiesemann, Zanderighi & Zanoli, 2204.00663]

Non-factorisable contributions

Q_{bG} corrections implemented into POWHEG-BOX. Possible to obtain realistic exclusive description of pp → Zh → $l^+l^-b\bar{b}$ production with NNLO accuracy using MiNLO′ & $\text{MiNNLO}_{\text{PS}}$ methods. Applying code to Higgs decay leads to:

$$\Gamma(h \to b\bar{b})^{\text{non}}_{\text{SMEFT}} = \frac{3y_b^2 m_h}{16\pi}\left(\frac{\alpha_s}{\pi}\right)^2 \frac{m_h^2}{3v^2}\left[1 + \frac{\alpha_s}{\pi}17.32\right]\frac{v^2}{\Lambda^2}\,\text{Re}\,(C_{bG})$$

new term represents
a 60% correction

[see MiNNLO talks on Tuesday morning; UH, Scott, Wiesemann, Zanderighi & Zanoli, 2204.00663]

Contributions from Q_{HG}

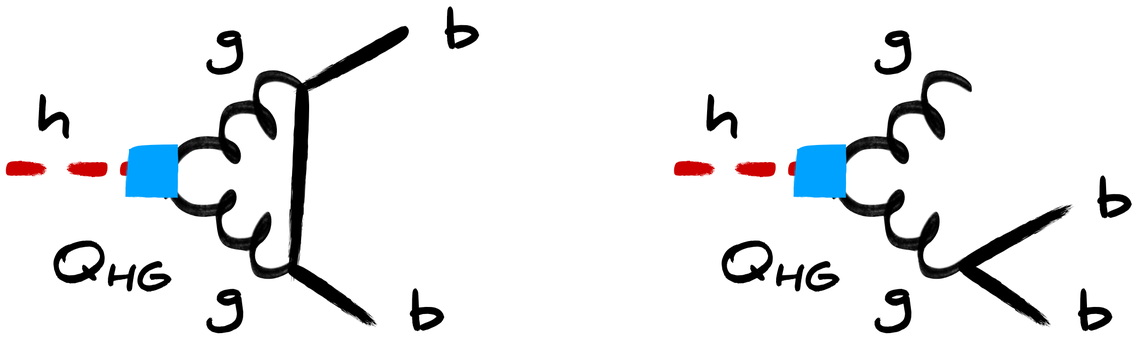

$$c_{HG} = \frac{v^2}{\Lambda^2} C_{HG} \in [-0.09, 0.06]$$

[Ellis et al., 2012.02779]

$$\frac{\Gamma(h \to b\bar{b})^{HG}_{\text{SMEFT}}}{\Gamma(h \to b\bar{b})^{\text{LO}}_{\text{SM}}} = \left(\frac{\alpha_s}{\pi}\right)^2 \left[\frac{19}{3} - 2\zeta_2 + \frac{1}{3}\ln^2\left(\frac{m_b^2}{m_h^2}\right)\right] c_{HG} \in [-2.7, 1.7] \cdot 10^{-3}$$

[Gauld, Pecjak & Scott, 1607.06354; UH, Scott, Wiesemann, Zanderighi & Zanoli, 2204.00663]

Contributions from Q_{HG}

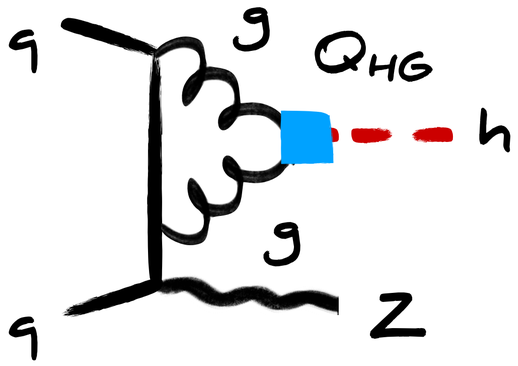

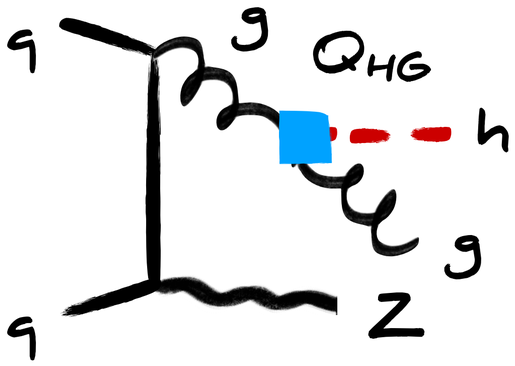

$$c_{HG} = \frac{v^2}{\Lambda^2} C_{HG} \in [-0.09, 0.06]$$

[Ellis et al., 2012.02779]

$$\frac{\sigma(pp \to hZ)^{HG}_{\text{SMEFT}}}{\sigma(pp \to hZ)^{\text{LO}}_{\text{SM}}} = 3 \left(\frac{\alpha_s}{\pi}\right)^2 \delta\, c_{HG} \in [-3.9, 2.4] \cdot 10^{-3}$$

numerically, one has δ = 10.7

[Brein, Harlander, Wiesemann & Zirke, 1111.0761; UH, Scott, Wiesemann, Zanderighi & Zanoli, 2204.00663]

Contributions from Q_{3G}

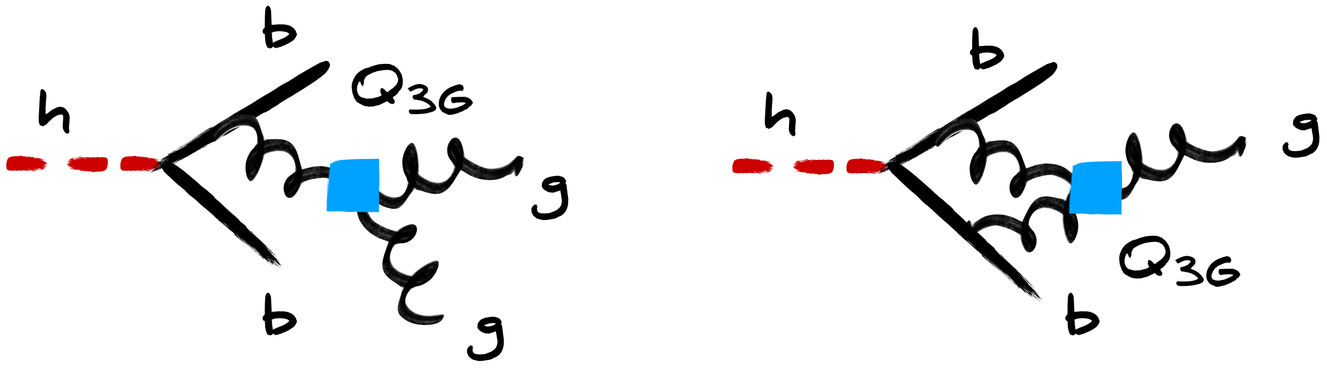

$$c_{3G} = \frac{v^2}{\Lambda^2} C_{3G} \in [-12.5, -4.1]$$

[Ellis et al., 2012.02779]

$$\frac{\Gamma(h \to b\bar{b})^{3G}_{\text{SMEFT}}}{\Gamma(h \to b\bar{b})^{\text{LO}}_{\text{SM}}} = N^{\text{dec}}_{3G} \left(\frac{\alpha_s}{\pi}\right)^2 \frac{m_h^2}{v^2} c_{3G} \in [-0.3, -0.1] \cdot 10^{-3}$$

explicit calculation gives $N^{\text{dec}}_{3G} = 2.23$

[UH, Scott, Wiesemann, Zanderighi & Zanoli, 2204.00663]

Contributions from Q_{3G}

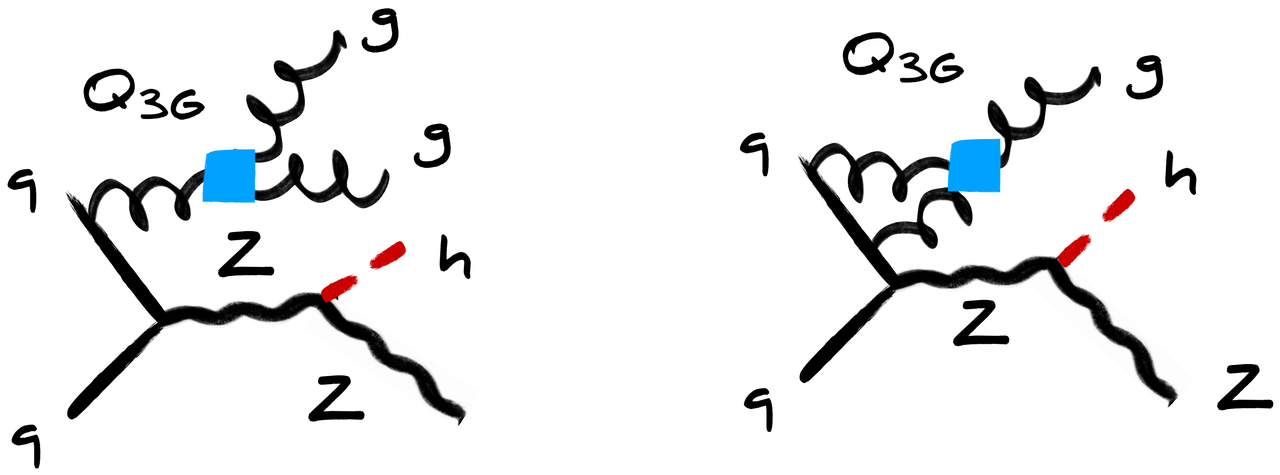

$$c_{3G} = \frac{v^2}{\Lambda^2} C_{3G} \in [-12.5, -4.1]$$

[Ellis et al., 2012.02779]

$$\frac{\sigma(pp \to hZ)^{3G}_{\text{SMEFT}}}{\sigma(pp \to hZ)^{\text{LO}}_{\text{SM}}} = N_{3G}^{\text{prod}} \left(\frac{\alpha_s}{\pi}\right)^3 c_{3G} \in [-5.8, -1.9] \cdot 10^{-3}$$

quoted number corresponds to $N_{3G}^{\text{prod}} = 10$

[UH, Scott, Wiesemann, Zanderighi & Zanoli, 2204.00663]

Phenomenology analysis

We have seen that QCD corrections associated to operators other than $Q_{H\Box}$, Q_{HD}, Q_{bH} & Q_{bG} do not exceed level of a few permille

Maximal size of factorisable corrections to partial h → $b\bar{b}$ decay rate can be derived from global fits of SMEFT Wilson coefficients:

$$\frac{\Gamma(h \to b\bar{b})^{\mathrm{N^3LO}}_{\mathrm{SMEFT}}}{\Gamma(h \to b\bar{b})^{\mathrm{N^3LO}}_{\mathrm{SM}}} - 1 \;\in\; [-39, 26]\% \quad \text{for} \quad c_{bH} = \frac{v^2}{\Lambda^2}\,\mathrm{Re}(C_{bH}) \in [-0.13, 0.20]$$

[Ellis et al., 2012.02779]

Phenomenology analysis

factorisable contributions just lead to a constant shift, i.e. a K-factor, in all $pp \to Zh \to l^+l^-b\bar{b}$ distributions

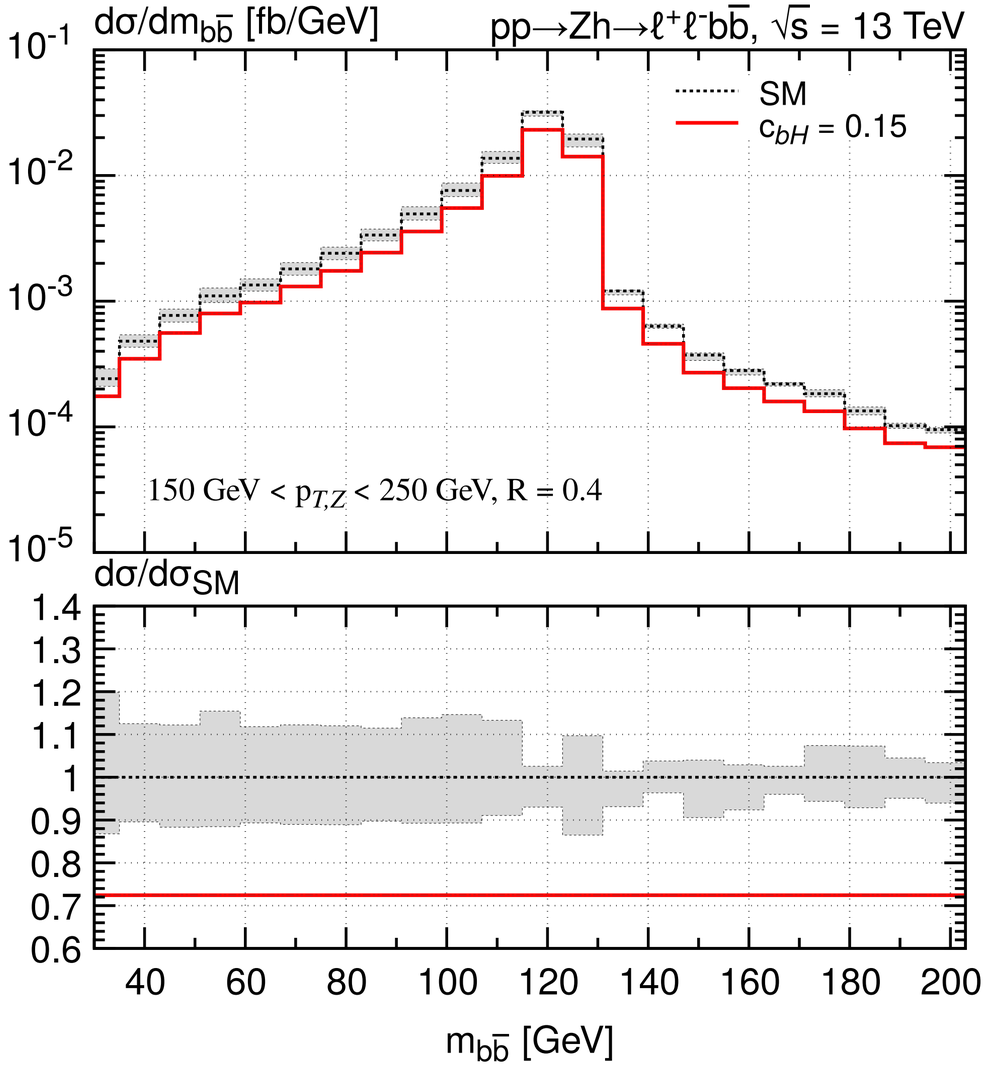

[UH, Scott, Wiesemann, Zanderighi & Zanoli, 2204.00663]

Interlude: bounds on dipole operator Q_{bG}

Observable	Wilson coefficient	95% CL bound
Dijet angular distributions	$\left\lvert c_{bG} \right\rvert$	2864
Two b-tagged jets	$\left\lvert c_{bG} \right\rvert$	152
Z-boson production with two b-jets	$\left\lvert c_{bG} \right\rvert$	438
Searches for neutron electric dipole moment	$\left\lvert \mathrm{Im}\left(c_{bG}\right) \right\rvert$	0.05

Due to chirality-flipping nature of Q_{bG} no interference between SMEFT & SM amplitudes for $m_b = 0$. Resulting LHC bounds on $|c_{bG}|$ thus very weak. $|\mathrm{Im}(c_{bG})|$ instead severely constrained by neutron electric dipole moment

[UH & Koole, 2106.01289]

Phenomenology analysis

Despite large Wilson coefficient of Q_{bG} possible size of non-factorisable contributions to partial $h \to b\bar{b}$ decay rate smaller than that of factorisable ones by a factor of O(5):

$$\frac{\Gamma(h \to b\bar{b})^{\mathrm{N^3LO}}_{\mathrm{SMEFT}}}{\Gamma(h \to b\bar{b})^{\mathrm{N^3LO}}_{\mathrm{SM}}} - 1 \in [-6.3, 6.3]\% \text{ for } c_{bG} = \frac{v^2}{\Lambda^2}\,\mathrm{Re}(C_{bG}) \in [-438, 438]$$

But non-factorisable contributions lead to non-trivial modifications of spectra in $pp \to Zh \to l^+l^-b\bar{b}$ production

Phenomenology analysis

extra gluon emission in leading-order Q_{bG} contribution tends to reduce dibottom invariant mass relative to SM

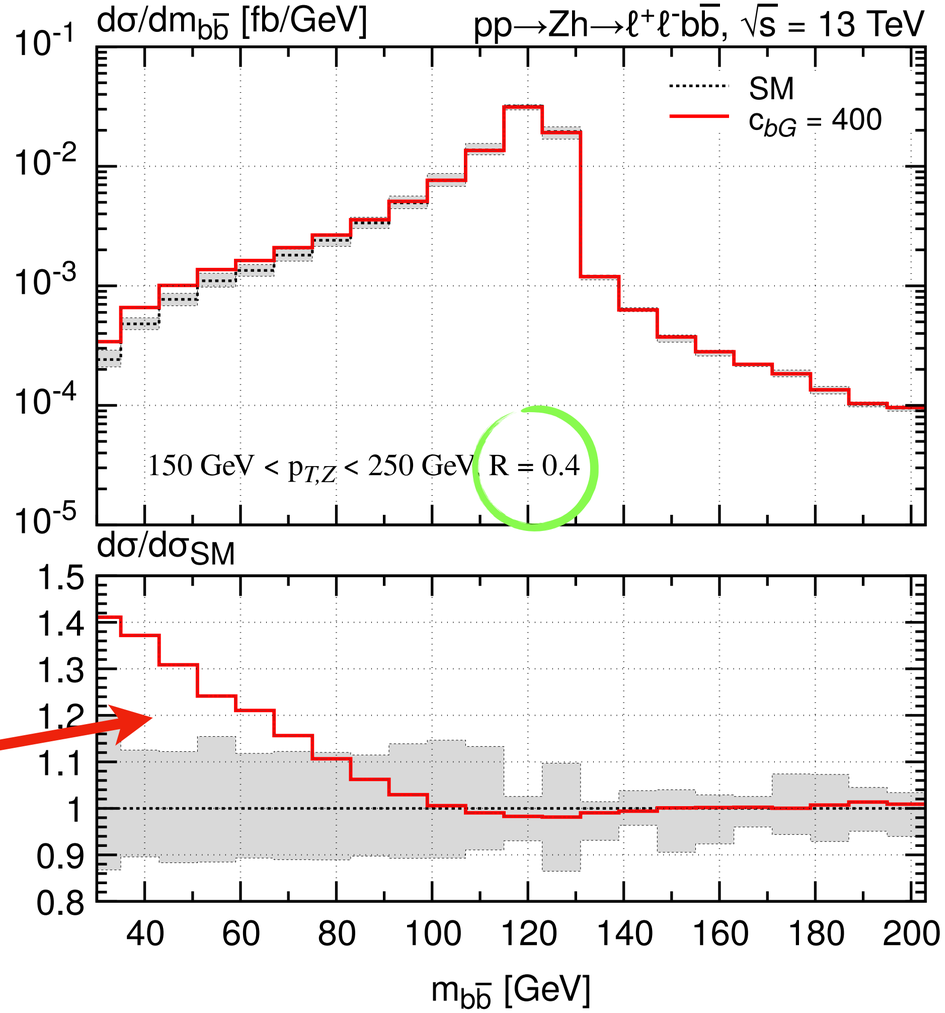

[UH, Scott, Wiesemann, Zanderighi & Zanoli, 2204.00663]

Phenomenology analysis

size of effect depends on radius parameter R used to reconstruct anti-k_t jets

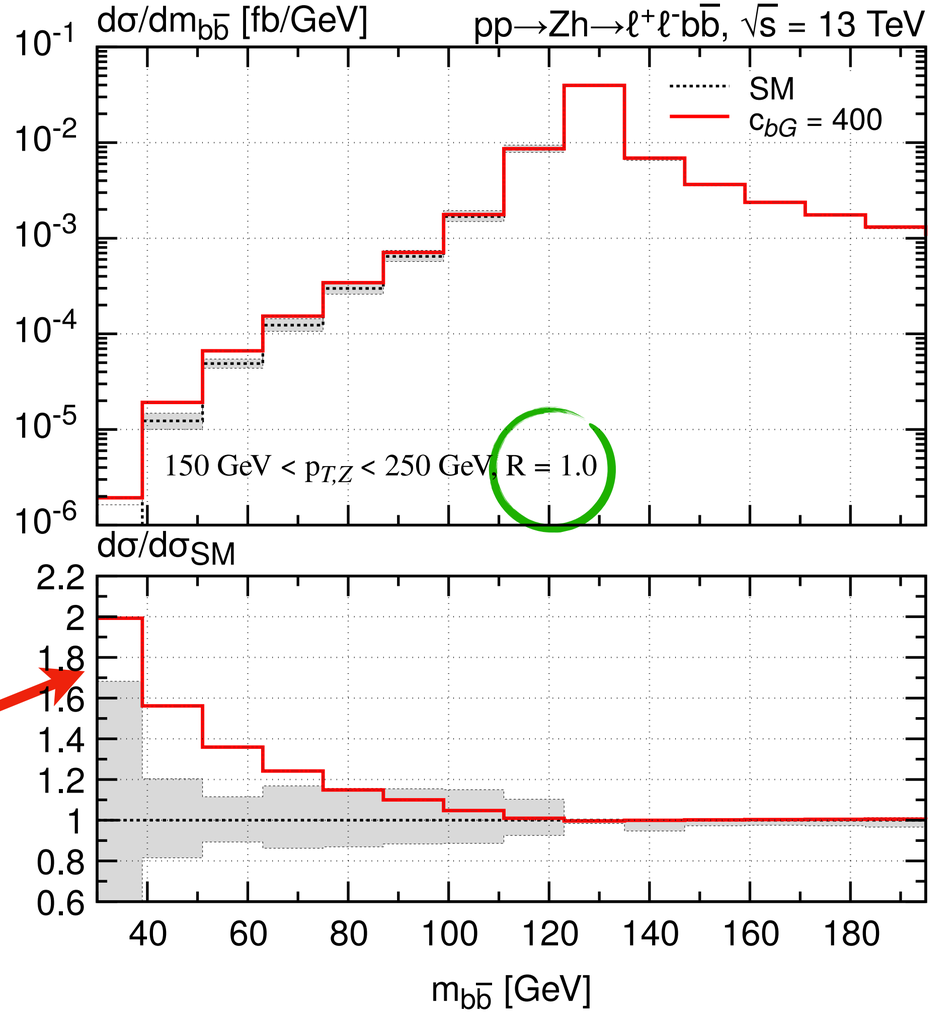

[UH, Scott, Wiesemann, Zanderighi & Zanoli, 2204.00663]

Phenomenology analysis

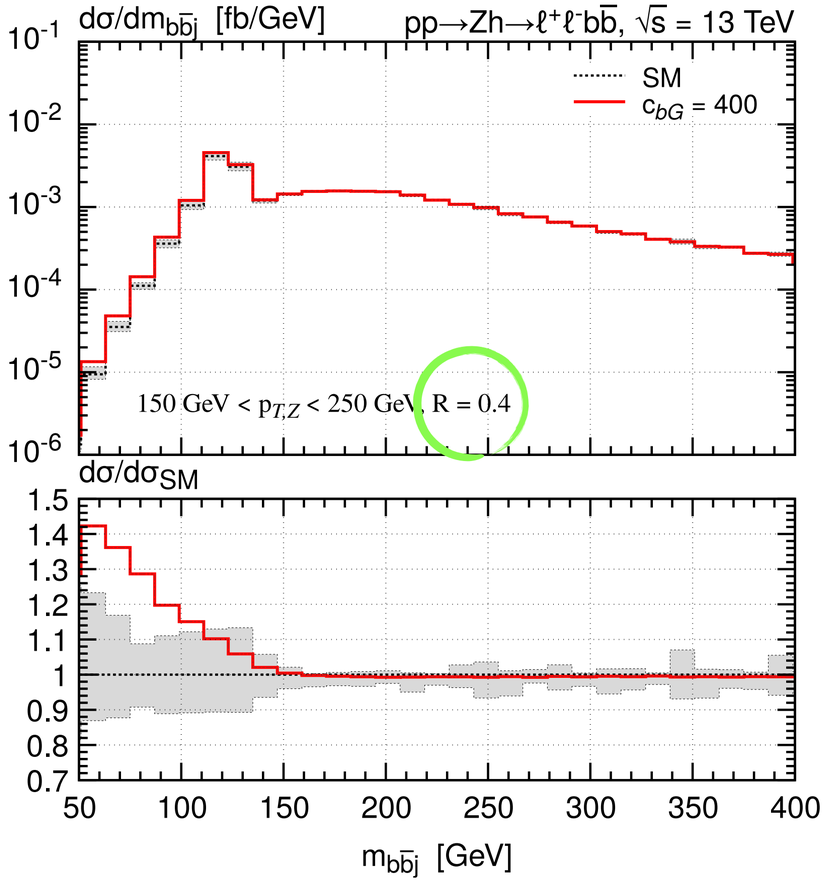

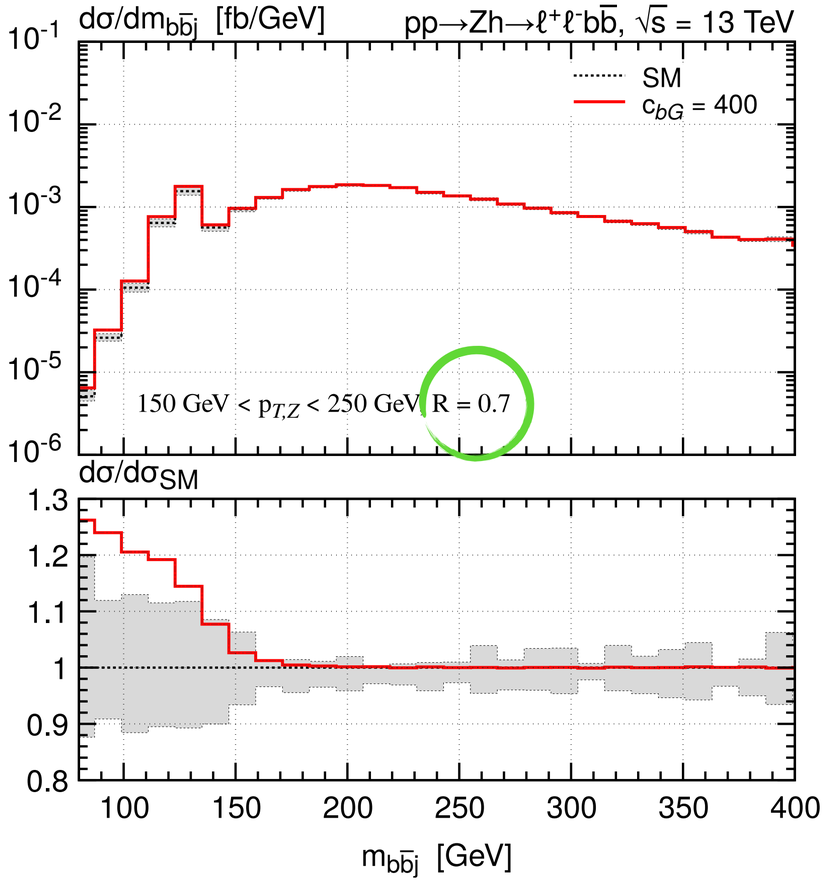

Also 3-jet invariant mass reduced on average. Effects again R-dependent

[UH, Scott, Wiesemann, Zanderighi & Zanoli, 2204.00663]

Outlook

Non-trivial shape changes of distributions in $pp \to Zh \to l^+l^-b\bar{b}$ production in combination with R-dependence may allow to enhance sensitivity to dipole operator Q_{bG} which is presently only very weakly constrained

Further opportunities at a e^+e^- machine using event shapes

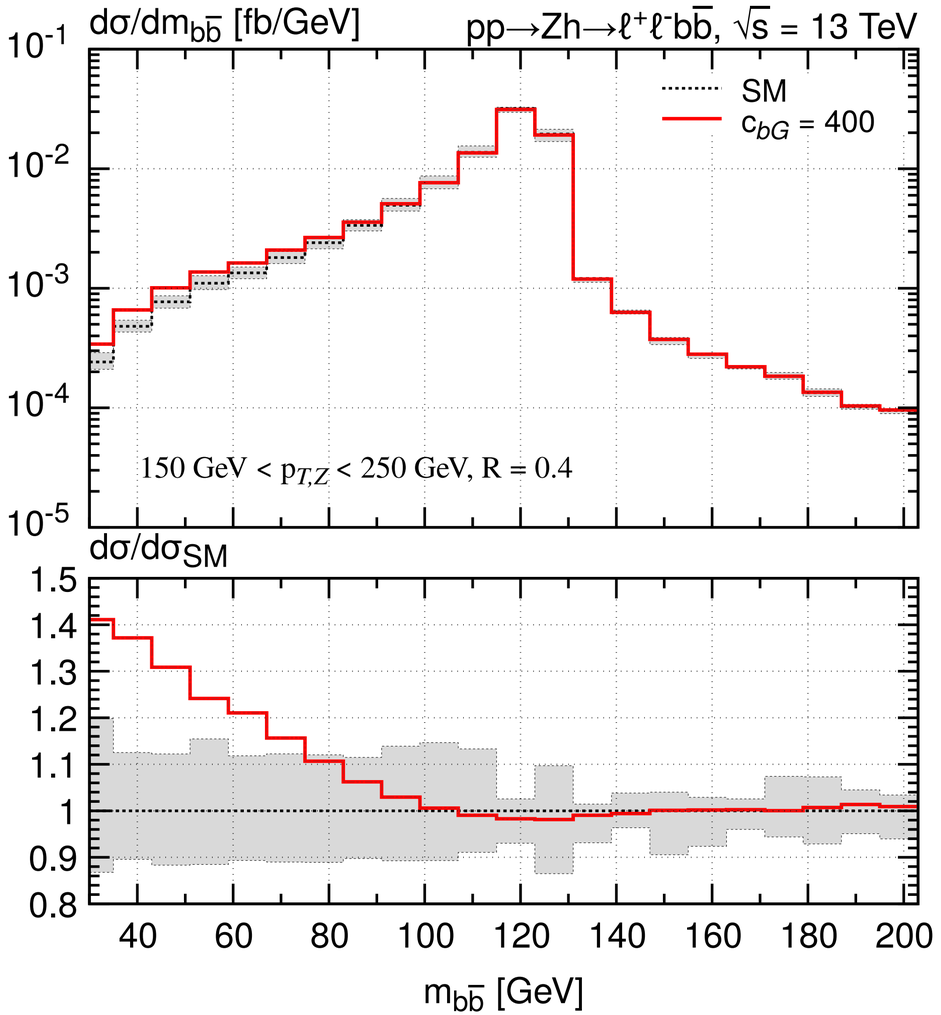

Outlook

Inclusion of EW SMEFT operators that modify hZZ vertex straightforward since full information already encoded in SM Drell-Yan amplitudes

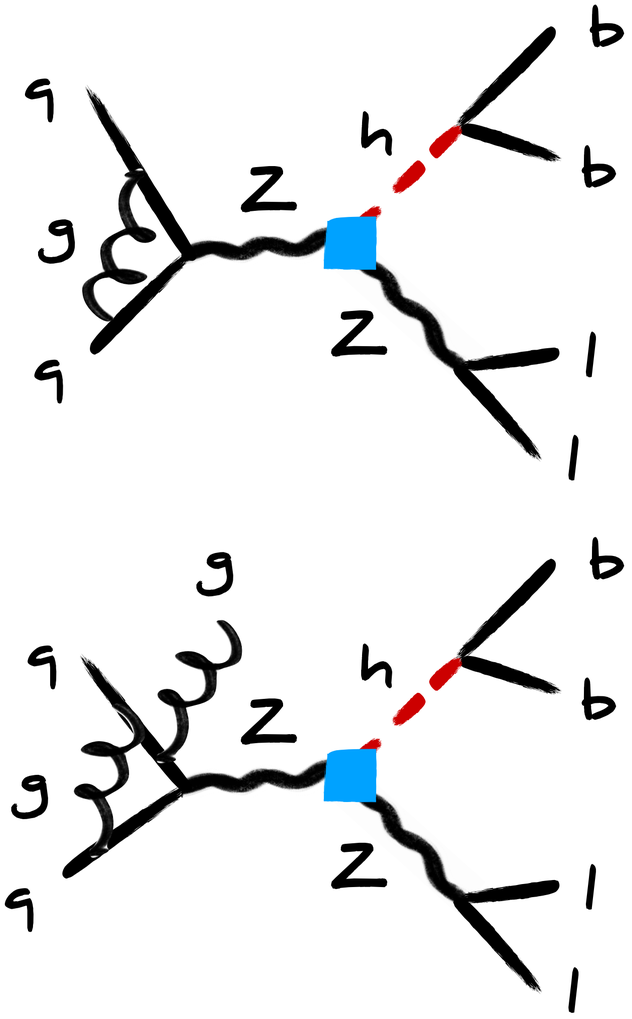

Outlook

Same is true for QCD corrections involving SMEFT operators modifying $q\bar{q}Z$ & $q\bar{q}Zh$ vertices

NNLO+PS implementation of dominant contributions from EW SMEFT operators in POWHEG-BOX framework ongoing. Stay tuned!

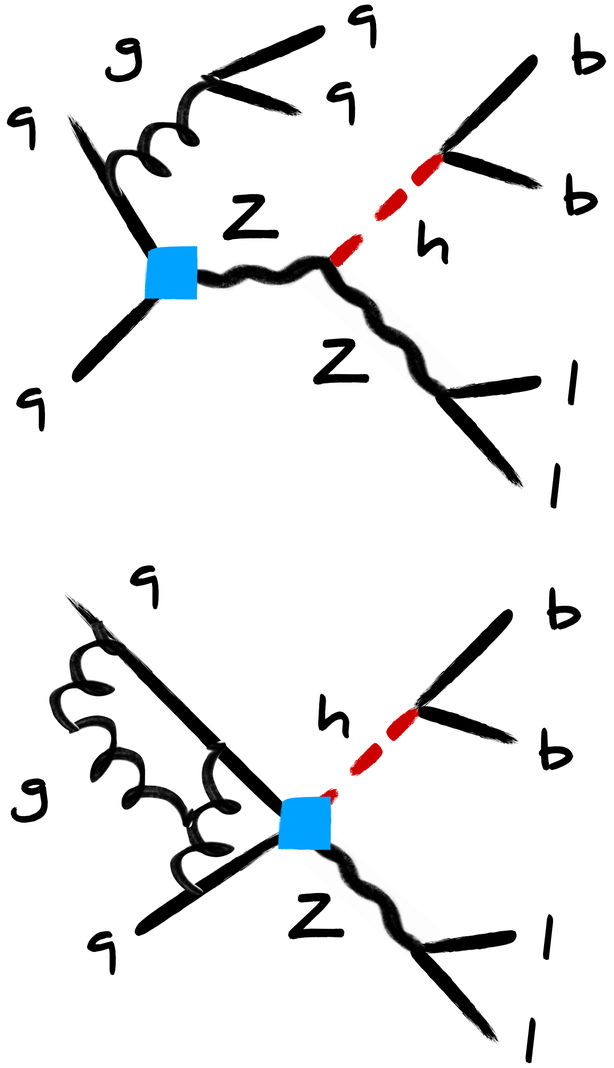

Backup

SMEFT corrections to total Higgs width

$$\Gamma_h^{\text{SMEFT}} = \left(1 + 2c_{\text{kin}}\right)\left[\Gamma_h^{\text{SM}} - \left(2\Delta c_{bH} - K_{bG}\,\Delta_{\text{non}}\,c_{bG}\right)\Gamma(h \to b\bar{b})^{\text{LO}}_{\text{SM}}\right.$$

$$\left. + 6K_{HG}\,c_{HG}\,\Gamma(h \to gg)^{\text{LO}}_{\text{SM}}\right]$$

$K_{HG} = 1.844$

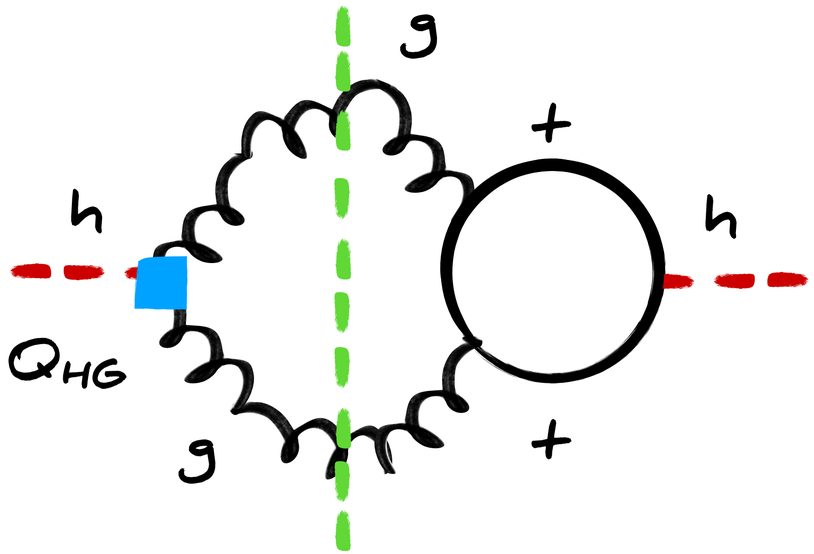

[UH, Scott, Wiesemann, Zanderighi & Zanoli, 2204.00663]

Event selections

In our differential analysis we select events with two charged leptons (electrons or muons) to explore the $Zh \to \ell^+\ell^- b\bar{b}$ signature. The leptons are required to have a transverse momentum of $p_{T,\ell} > 15\,\text{GeV}$ and a pseudorapidity of $|\eta_\ell| < 2.5$. The invariant mass of the dilepton pair is restricted to $m_{\ell^+\ell^-} \in [75, 105]\,\text{GeV}$. The events are furthermore required to have at least two b-jets, which are reconstructed using the anti-k_t algorithm [65] as implemented in `FastJet` [66]. We impose transverse momentum cuts of $p_{T,b} > 25\,\text{GeV}$ and a rapidity threshold of $|\eta_b| < 2.5$ on the b-jets. The definition of potential additional jets use the same thresholds as those of the b-jets. The dominant background processes are Z + jets, $t\bar{t}$, single-top and diboson production. The latter three types of backgrounds can be substantially reduced by requiring large values of $p_{T,Z}$ [67]. Hence, to improve the signal-to-background ratio we impose $p_{T,Z} \in [150, 250]\,\text{GeV}$. Notice that this $p_{T,Z}$ requirement corresponds to the second resolved $p_{T,Z}$ bin as recommended in the stage 1.2 simplified template cross sections (STXS) framework [68–70] which is also implemented in the latest ATLAS LHC Run II measurements of the $pp \to Zh \to \ell^+\ell^- b\bar{b}$ process [71, 72]. We will also comment on how our results are modified if the other two resolved regions, i.e. $p_{T,Z} \in [75, 150]\,\text{GeV}$ and $p_{T,Z} > 250\,\text{GeV}$, are considered.

[UH, Scott, Wiesemann, Zanderighi & Zanoli, 2204.00663]

Bounds on dipole-type operator Q_{bG}

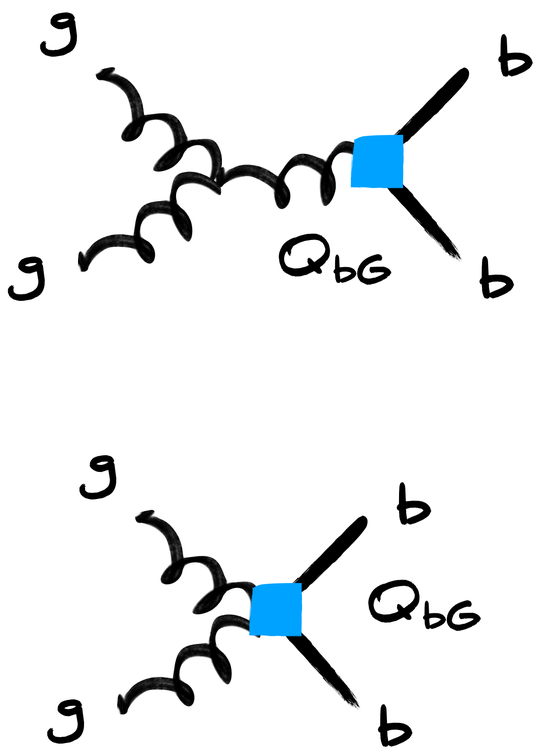

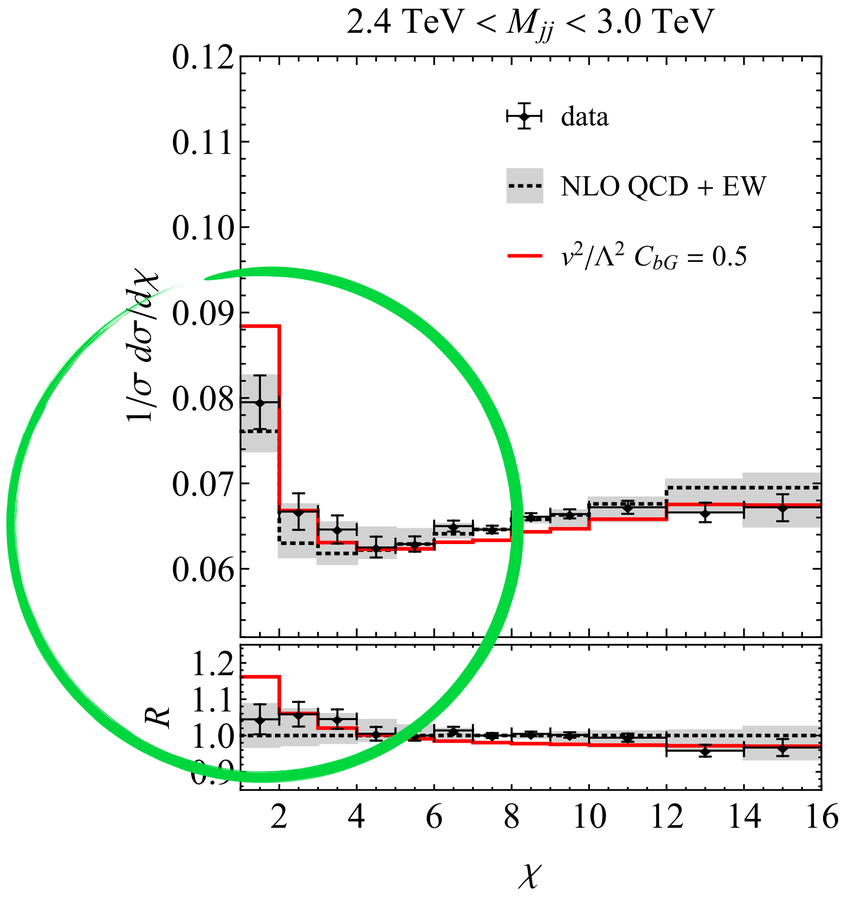

Q_{bG} contributions lead to an enhanced activity of high-energy jets in central region

[UH & Koole, 2106.01289]

Bounds on dipole-type operator Q_{bG}

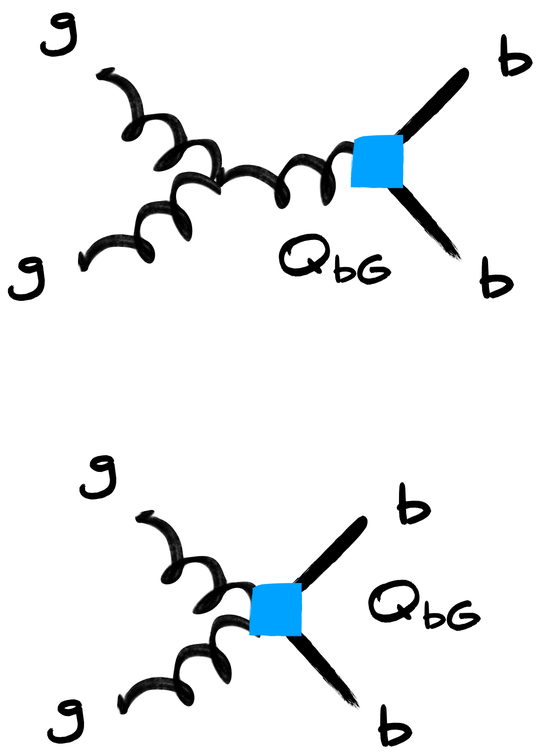

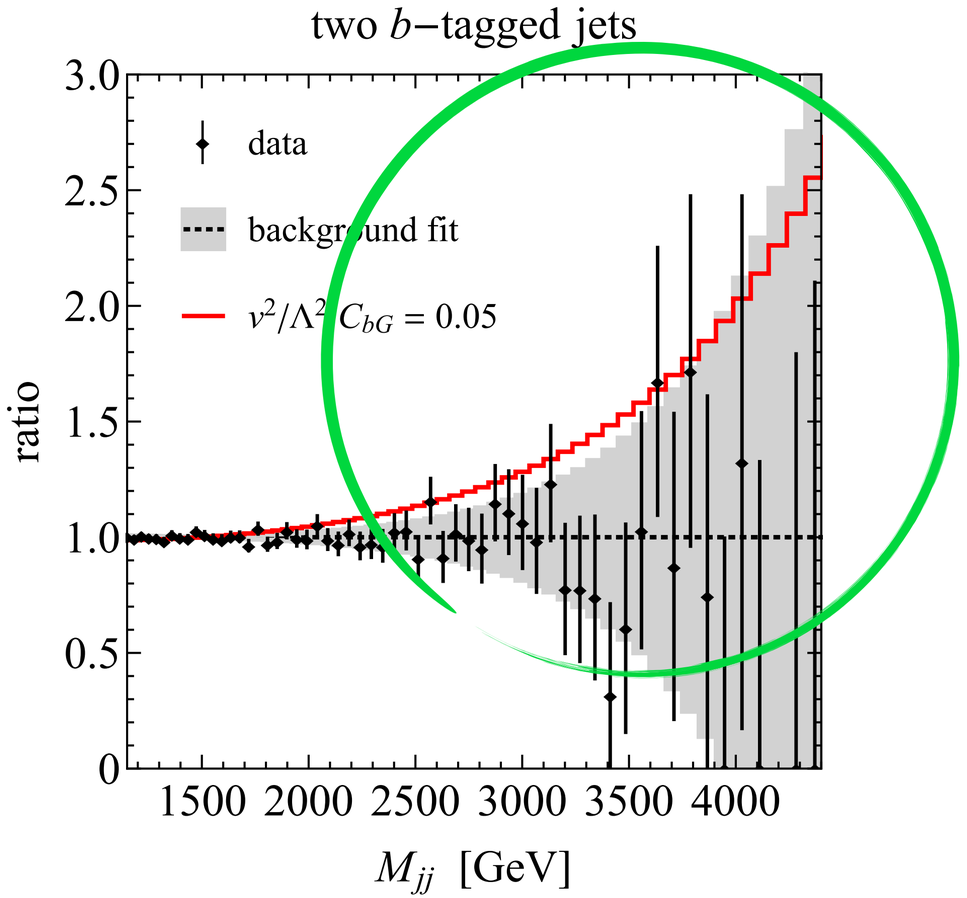

Q_{bG} contributions lead to an enhancement of rate for high dijet invariant masses

[UH & Koole, 2106.01289]

Bounds on dipole-type operator Q_{bG}

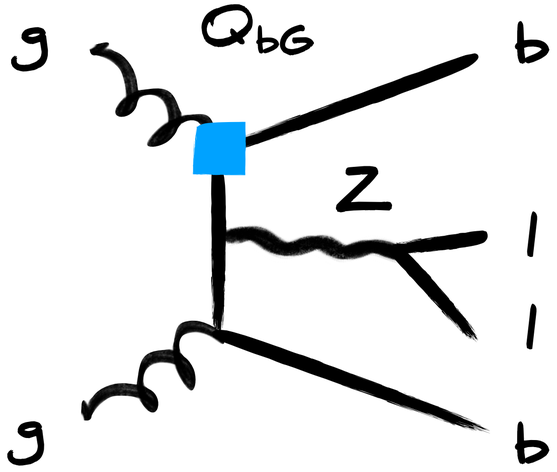

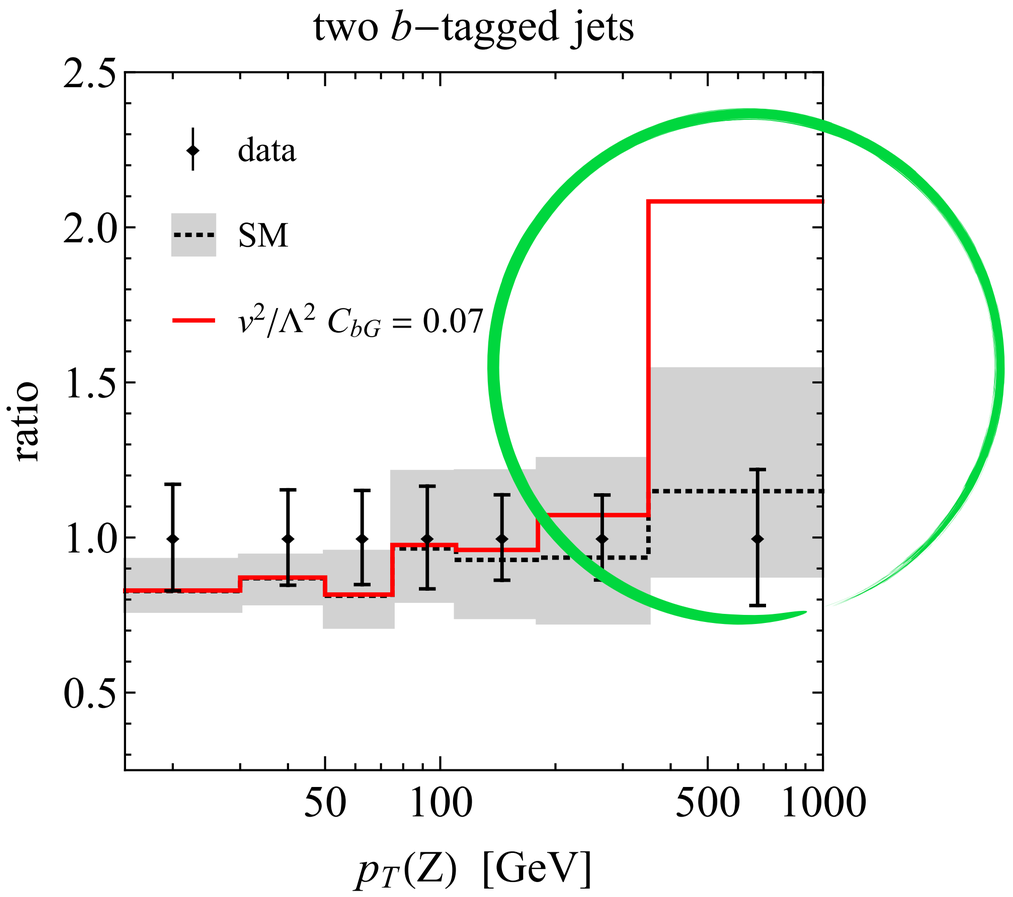

Q_{bG} effects grow with transverse momentum & lead to more events at high $p_T(Z)$

[UH & Koole, 2106.01289]

Bounds on dipole-type operator Q_{bG}

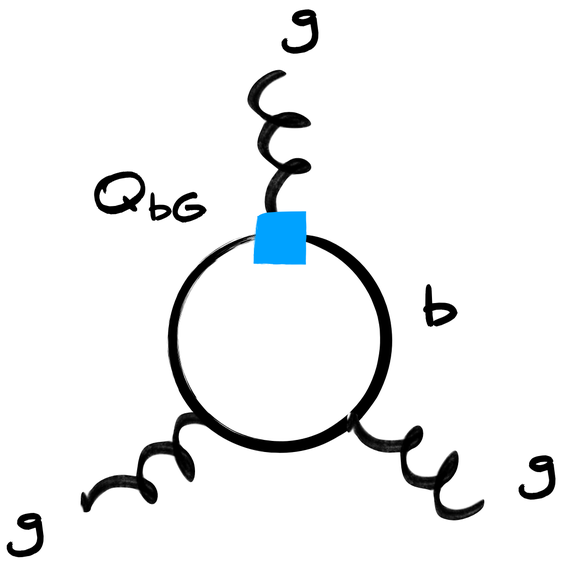

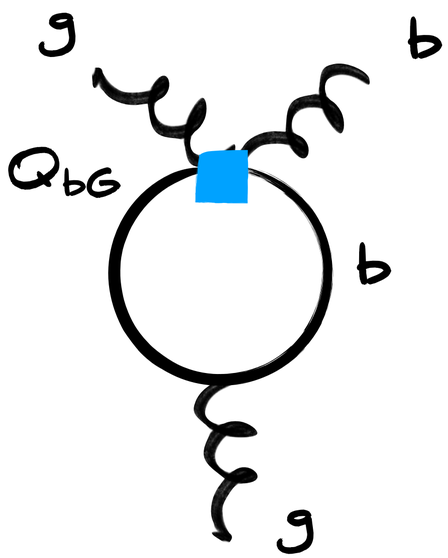

$$f^{abc} G^{a}_{\mu\sigma} G^{b,\sigma}_{\nu} \widetilde{G}^{c,\mu\nu}$$

1-loop threshold corrections involving Q_{bG} generate CP-violating Weinberg operator.

This operator leads to a non-zero neutron electric dipole moment at hadronic scale

[UH & Koole, 2106.01289]

ZZh operators

$$\mathcal{L} = -\frac{1}{4\Lambda} g^{(1)}_{hZZ} Z_{\mu\nu} Z^{\mu\nu} h$$
$$- \frac{1}{\Lambda} g^{(2)}_{hZZ} Z_{\nu} \partial_{\mu} Z^{\mu\nu} h$$
$$- \frac{1}{4\Lambda} \tilde{g}_{hZZ} Z_{\mu\nu} \tilde{Z}^{\mu\nu} h$$

Setup 1: $g^{(1)}_{hZZ} = 2.8\,,\ g^{(2)}_{hZZ} = -0.6$

Setup 2: $g^{(1)}_{hZZ} = 1.05\,,\ \tilde{g}_{hZZ} = -2.9$

[Bizon et al., 2106.06328]

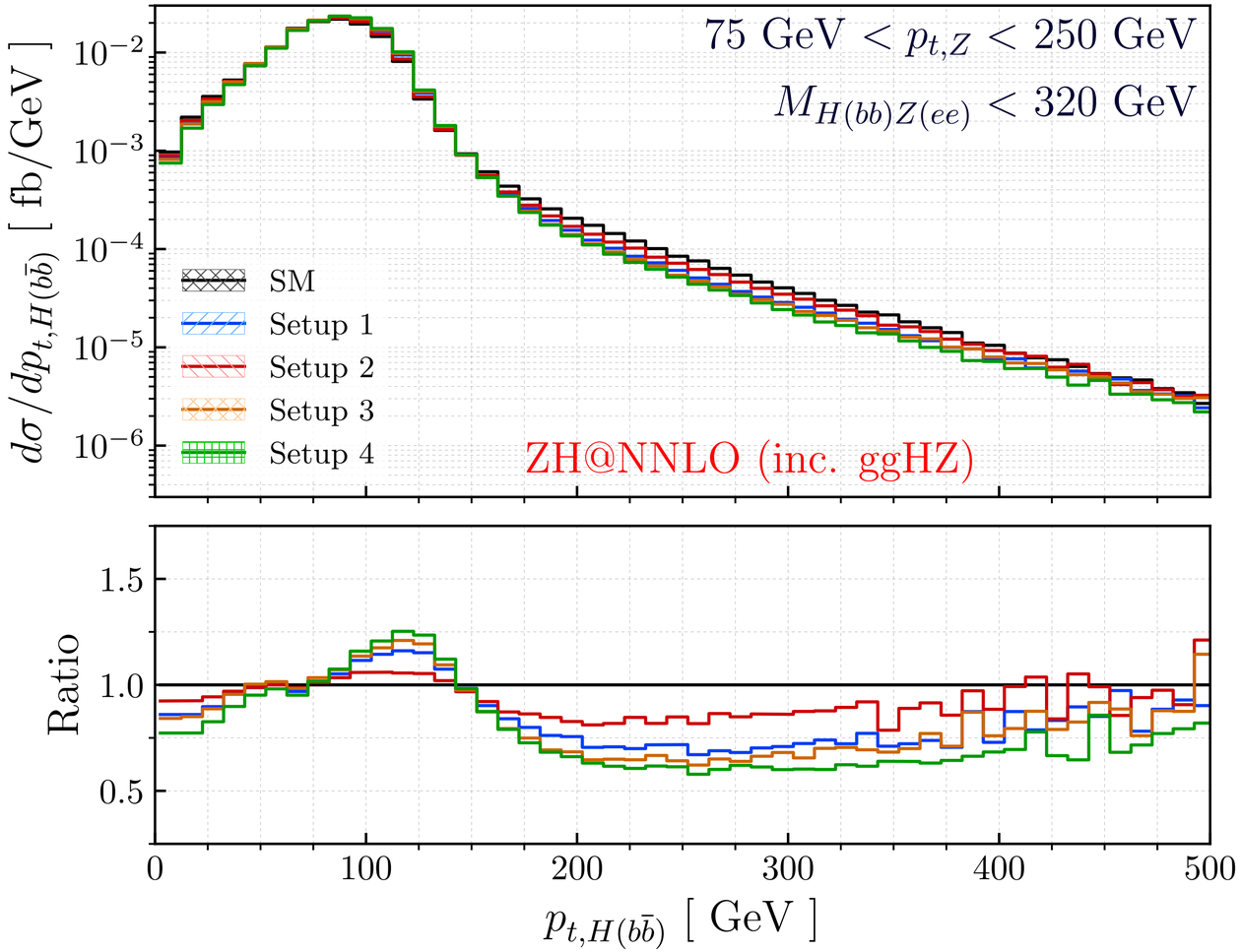

ZZh operators lead to shape changes in kinematic spectra of pp → Zh → $l^+l^-b\bar{b}$

qq̄Z & qq̄Zh operators

$$Q_{Hq}^{(1)} = \bar{q}_L \gamma^\mu q_L \left(i H^\dagger \overleftrightarrow{D}_\mu H \right) \, , \ldots$$

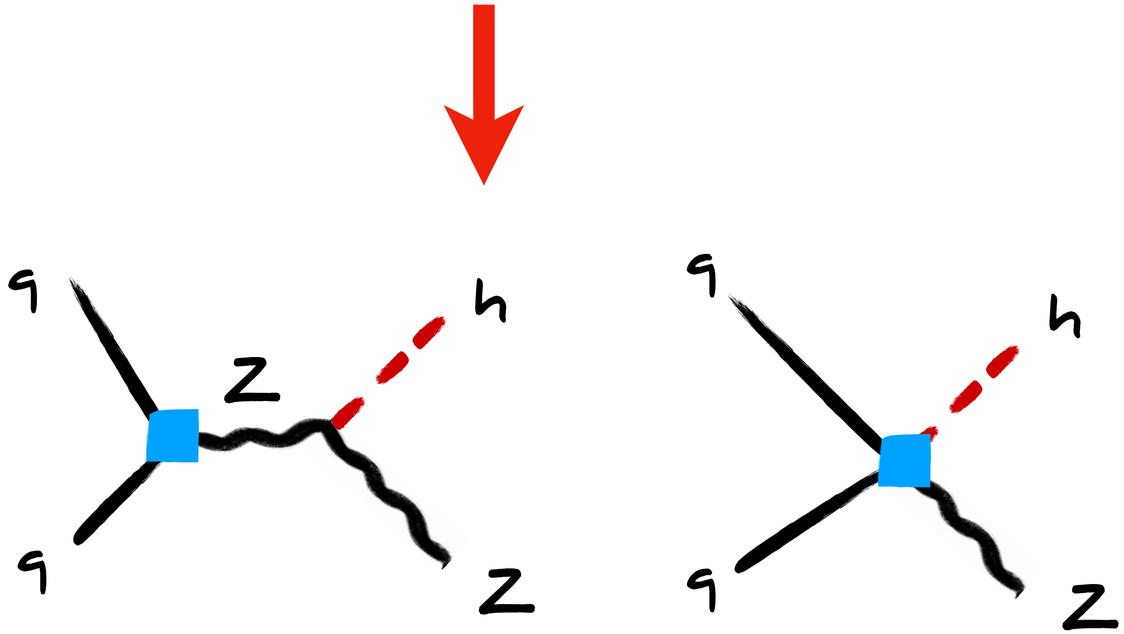

modifications grow with energy, making Zh searches @ LHC in boosted regime competitive with LEP bounds on Z couplings

$$\propto \frac{(p_Z + p_h)^2}{M_Z^2}$$

[see for instance Bishara et al., 2208.11134]